Magnetic X-ray circular dichroism on *in situ* grown 3*d* magnetic thin films on surfaces

Dimitri Arvanitis,[a]* Jonathan Hunter Dunn,[b] Olof Karis,[a] Anders Hahlin,[a] Barbara Brena,[a] Roger Carr[b] and Nils Mårtensson[a]

[a]Physics Department Uppsala University, Box 530, S-75121 Uppsala, Sweden, and [b]Stanford Synchrotron Radiation Laboratory, SLAC, Stanford University, Stanford, CA 94309, USA. E-mail: dimitri.arvanitis@fysik.uu.se

Epitaxic thin and ultrathin films on surfaces allow crystallographic phases that do not occur naturally in the bulk to be stabilized. They also offer new possibilities for an improved understanding of soft X-ray photoabsorption in magnetic systems. Data collected using the Elliptically Polarizing Undulator at BL 5.2 of the Stanford Synchrotron Radiation Laboratory are presented herein. Fe, Co and Ni films were prepared on Cu(100) surfaces. $L_{2,3}$-edge spectra were recorded with circular and linear light. Fresnel diffractometry was used to quantify the degree of transverse beam coherence. A quantitative analysis of the spectral features indicates a correlation of the spectral intensities and the transverse beam coherence. Resonant reflectivity spectra for Co ultrathin films that exhibit strong dichroism are presented. The reflectivity data indicate that interference effects of the reflected beams at the two interfaces are of importance, even for ultrathin films.

Keywords: epitaxic film; magnetic moment; transverse coherence; resonant reflectivity.

1. Introduction

Ultrathin ferromagnetic films can be prepared and characterized using surface-science-based techniques. Here we focus on such systems prepared and characterized *in situ* under ultra-high vacuum (UHV) conditions. High brightness X-ray sources can be used to measure the magnetic properties of dilute systems relevant for technological applications (for a recent review see, *e.g.* Kortright *et al.*, 1999). In contrast to most technology-oriented research, we do not make use of cap layers, as these very often affect several of the properties of ultrathin films, such as the Curie temperature or the saturation magnetization (May *et al.*, 1997). Despite the complication of such *in situ* studies, we show that they possess a prototypical character, leading to a better understanding of magnetism and photoabsorption at low dimensions.

During the past decade, measurements have been performed on *in situ* prepared ultrathin films in the photoabsorption mode (electron yield or photocurrent) at second-generation facilities, such as BESSY I (Berlin, Germany) and MAX-I (Lund, Sweden). Out-of-plane dipole radiation was used to generate circular X-rays. Here we present experiments performed at the Stanford Synchrotron Radiation Laboratory (SSRL) using the Elliptically Polarizing Undulator (EPU) and BL 5.2. This source can produce circular X-rays of much higher brilliance as compared to out-of-plane dipole radiation at second-generation facilities. In particular, studies of face-centred tetragonal (f.c.t.) Ni and Co ultrathin films on single-crystal Cu surfaces by means of *L*-edge element-specific magnetometry are reported herein. Magnetic circular X-ray dichroism (MCXD) experiments were performed using circular X-rays, allowing the empty final states at a specific atomic site to be probed spin-selectively. Sum rules established for MCXD spectra yielded the ground-state expectation value of the orbital and spin magnetic moments of the core-excited atom (Carra *et al.*, 1993). To derive these, several approximations were made. In particular, an atom-like model was assumed to describe the nature of the electron final states, as well as an infinite source coherence of the exciting radiation.

In previous MCXD measurements, we concentrated on the characterization of the magnetic properties of ultrathin films of Fe, Co and Ni on a Cu(100) substrate. In the case of the ultrathin Co/Cu(100) films (Tischer *et al.*, 1994), the temperature dependence of the MCXD difference was investigated for thicknesses between 1.5 and 2.1 ML (ML = monolayer). Determining magnetic moments as a function of film thickness (50 to 1.5 ML) and temperature, established an enhancement of the orbital moment of the surface Co atoms by 100% as compared to the bulk (Tischer *et al.*, 1994, 1995). The careful characterization of the MCXD response for these films as a function of temperature, film thickness and X-ray incidence angle enabled the quantification of saturation effects (Hunter Dunn *et al.*, 1995). Enhanced orbital and spin moments for the f.c.t. phase, as compared to the body-centred cubic (b.c.c.) bulk, were found by means of an MCXD angle-dependent study of the f.c.t. and b.c.c. phases for Fe/Cu(100) (Hunter Dunn *et al.*, 1996). Enhanced magnetic moments were also measured from the topmost layers of the thicker b.c.c. Fe/Cu(100) films. Magnetism-related energy shifts and broadenings were measured for the b.c.c. and f.c.t. phases of Fe/Cu(100). These shifts could be related to the exchange splitting of the *d* bands for these systems (Hunter Dunn *et al.*, 1996). Finally, the interaction of oxygen with thin Ni films has been studied. One is able to follow the charge flow from the Ni to the O atoms. The observed variations in the spectra at both edges enable a precise spectral assignment of *s* states and a calibration of the number of 3*d* holes (May *et al.*, 1996).

2. Experimental

We present experiments performed at the SSRL using the EPU and BL 5.2 (Carr *et al.*, 1995). The EPU in combination with BL 5.2 is capable of producing high-brilliance linear or circular soft X-ray light in the spectral range 0.5–1.5 keV. This source allows, in particular, the light helicity to be varied or the polarization state of the X-ray light to be varied without having to move optical elements in the beamline. Varying the position of optical elements, or having light beams not following the same optical path, often leads to different background and stray light contributions, adding adjustable parameters in the analysis of the photoabsorption spectra. We use the EPU in a 'static' mode, *i.e.* maintaining a fixed polarization for each spectrum. Several channels are recorded simultaneously: (i) the electron yield of the sample measured by means of a channel plate detector positioned below the sample; (ii) the sample photocurrent; (iii) the reflected beam intensity for the grazing angles of incidence, by means of an X-ray sensitive photodiode; (iv) the photocurrent from a fine Au mesh in the beam path (I_0 monitor). The diode and channel plate detector can be rotated about the polar axis independently of the sample rotation (Hunter Dunn, 1998).

The samples were remanently magnetized by means of magnetic field pulses, produced by a Helmholz coil pair that can also be rotated around the polar axis independently of the sample. By measuring the sharp La M_5 absorption resonance of an $LaAl_2$ standard, the energy resolution is characterized on-line at around 835 eV. The energy resolution of the data collected at BL 5.2, presented here, is found to be very similar to that of previous data on these systems recorded at BESSY I using the SX 700 III monochromator.

In a different type of experiment, the beam profile and diffraction patterns from obstacles on the beam path could be recorded by means of a mount consisting of an X-ray photodiode positioned behind an opaque shield with a 10 μm pinhole. This mount was positioned close to the sample on the sample rod. By recording the photodiode current and scanning this pinhole/photodiode assembly in the vertical plane across the X-ray beam, one is able to perform quantitative diffractometry at the sample position and characterize the transverse coherence of the X-ray beam *in situ*, under conditions identical to those used for the spectroscopic measurements. For the data collected at BL 5.2, tests were performed on the possible existence of low-energy stray light. By inserting various filters in the beam path, upstream from the measuring chamber but after monochromatization, both diffractometry and spectroscopy measurements were performed. No differences in spectral shape, edge-jump ratio or diffraction profile could be observed with the filters inserted.

The films were deposited *in situ* by means of electron beam evaporation, as described earlier (Hunter Dunn *et al.*, 1996). They were characterized, for order and cleanness, by means of low electron energy diffraction and photoabsorption at the C and O *K* edges. The film thickness was determined *in situ* by means of the edge-jump ratio (Arvanitis *et al.*, 1996; Hunter Dunn *et al.*, 1996); verification of a favourable film thickness was performed by means of Auger electron spectroscopy and the determination of the Curie temperature. The thin and ultrathin films evaporated on Cu(100) discussed here exhibit stable remanence and square hysteresis loops. This could be monitored *in situ* by recording the resonantly reflected light intensity *versus* magnetic field strength at the L_3 or L_2 edges of the overlayer. For the present set of data, we used typically field pulses of about 180 G to magnetize the samples along the easy direction. These fields were well in excess of the coercive field for all samples. As the coils can rotate independently of the sample, in a typical experimental geometry, the sample is rotated with the easy direction to couple with the photon spin under a given angle, the coils being rotated to deliver a field along the sample easy direction. With this setup, measurements can also be performed with the coils along the hard magnetic direction.

3. Discussion

3.1. *Magnetic moments and source coherence*

In order to measure the transverse source coherence, Fresnel diffractometry was performed *in situ*. The I_0 monitor Au mesh was used as an obstacle. Fig. 1 shows the photodiode current of the pinhole/photodiode assembly as the assembly is scanned across the shadow of the I_0 mesh in the vertical direction. The presented data were collected at SSRL BL 5.2, as well as at BL 22 of MAX-Lab (Lund, Sweden) using an SX 700 monochromator in an optical configuration similar to that used at BESSY. Clear Fresnel oscillations are seen in the case of BL 5.2 at an energy of 600 eV (Fig. 1, full line). A simple qualitative analysis of the data of Fig. 1 gives a transverse coherence of about 55 μm for BL 5.2 for this wavelength (20.6 Å). The measurements using the SX 700 monochromator (dashed line in Fig. 1) yield a transverse beam coherence of only 1.5 μm. In the two cases, the energy resolutions, which are linked to the longitudinal beam coherence, are very similar. Measurements of the La *M* resonances produce a value of about 1.5 eV for the Gaussian contribution (full width at half-maximum) of the monochromator resolution at 835 eV in both cases. The monochromator resolution improves at lower energies, following a power law. For the spectral range of interest here, the longitudinal coherence length is about 1 μm. Further details on the diffractometry measurements are given elsewhere (Hunter Dunn, Arvanitis, Baberschke *et al.*, 2000).

Figs. 2 and 3 show electron yield spectra for thicker Ni and Co films on Cu(100). These are shown at an angle of X-ray incidence that allows the photon spin to couple to the sample's remanence. In this thickness range, around 15–20 ML, the Ni films exhibit an out-of-plane remanence, while the Co films have an in-plane remanence. In both cases, the electron yield spectra were recorded at several angles of X-ray incidence, allowing saturation effects in the electron yield to be quantified and corrected, as presented elsewhere (Hahlin *et al.*, 2001). These spectra are shown after subtraction of a constant background, so the pre-edge is set to zero. The post-edge continuum is then set at 100 arbitrary units. The signal to background ratio in all cases is very good, yielding edge-jump ratios of the order of 250%. This enables a quantitative analysis even of small spectral details. By comparing the spectra of Figs. 2 and 3 taken at BL 5.2, with the data of similar samples taken at the SX 700 III of BESSY I (Arvanitis *et al.*, 1996), an enhancement of spectral features relative to the high-energy 'atomic' continuum is observed (Hahlin *et al.*, 2001). It is checked by convolving the BL 5.2 data with Gaussian profiles that the observed enhancement is not related to a variation of the photon energy resolution, associated with a relative suppression of the background *versus* the white-line intensity. This effect has been discussed previously for both thin and thick Fe films (Hunter Dunn, Arvanitis, Carr & Mårtensson, 2000; Hunter Dunn, Arvanitis, Baberschke *et al.*, 2000). A quantitative analysis of the strength of the saturation effects in the data collected at SSRL and BESSY for thicker Fe, Co and Ni films gives an independent measure of an increase of the white-line area for the data taken using the EPU at SSRL (Hahlin *et al.*, 2001). We propose a correlation between the intensity of spectral features and the transverse beam coherence. More details on this correlation are given elsewhere (Hunter Dunn, Arvanitis, Carr & Mårtensson, 2000; Hunter Dunn, Arvanitis, Baberschke *et al.*, 2000). Here we present mostly an analysis of the dichroic part of the spectra taken at SSRL and BESSY I. An enhancement of spectral features, correlating with the transverse source coherence, is of importance when the MCXD sum rules are

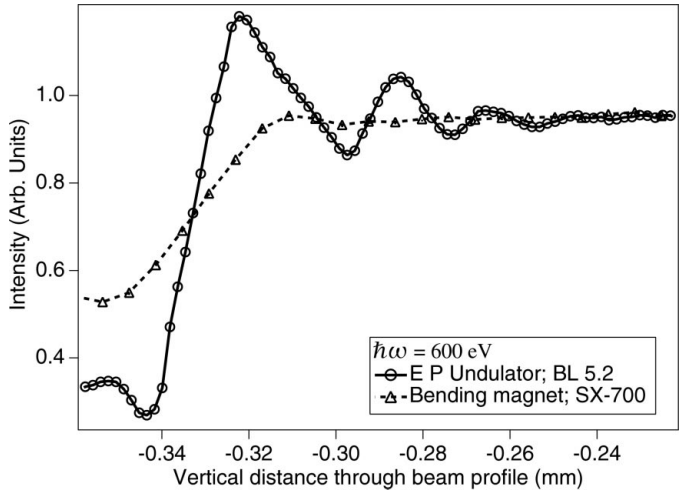

Figure 1
Fresnel diffraction from the I_0 monitor Au mesh in the beam path. In the case of the brighter source, at BL 5.2 of SSRL, clear Fresnel oscillations are recorded as one moves a pinhole-schielded photodiode in the shadow of the wires, across the vertical direction. No clear Fresnel oscillations are observed in the case of the less bright SX 700 dipole magnet source at MAX-Lab.

applied (Carra *et al.*, 1993), as one has to perform a quantitative analysis of white-line intensities.

The normalized MCXD difference spectra for the Co and Ni spectra of Figs. 2 and 3 are shown in Fig. 4 (full lines). For a complete comparison, we also present data from thick Fe films measured at BL 5.2 under the same conditions as discussed here (Hunter Dunn, Arvanitis, Carr & Mårtensson, 2000; Hunter Dunn, Arvanitis, Baberschke *et al.*, 2000). The corresponding data from BESSY (Arvanitis *et al.*, 1996) are also shown (dashed lines). To allow for a comparison, the spectra are normalized as in Figs. 2 and 3, as described above, in all cases. Given the fact that at BESSY a degree of circularity for the X-rays of 0.50 was used, while a degree of 0.95 was used at BL 5.2, the BESSY MCXD difference data have been rescaled by a factor in order to allow for a meaningful comparison of the dichroic parts of the spectra. Factors of 1.34, 1.04 and 1.43 were used for the Fe, Co and Ni data, respectively. These values correspond to the ratios of the spin moments as determined from these data, so that identical spin values are determined, as described below. From Fig. 4, we conclude (full *versus* dashed lines) that this does not correspond to a situation where the extreme values in the difference spectra at the L_3 and L_2 edges yield similar dichroic intensities. Good agreement between the BESSY and SSRL data is observed for all elements, in particular for the high-energy asymmetric tail above the L_2 edge. We also observe that there are small but systematic differences in the shape of the spectra in the energy region between the L_3 and L_2 lines. Previously this region was thought to correspond to transitions to final states of mostly *s* symmetry (May *et al.*, 1996).

Even if these differences appear at first glance small, they are significant. Given the spectral shape, these differences cannot be attributed to variations in the background signal that would be source dependent. This is easiest to see in Fig. 4 for Ni and Fe, and by more precise inspection for Co. For Ni, the dichroic satellite region above the L_3 line exhibits a different shape. Also, for Fe, more fine structure is observed above the L_3 line. A comparison of the L_3 and L_2 lines between the two sets of data also reveals that despite a very similar width for Ni, broader *L* lines are observed for Co at BESSY and even more so for Fe, despite a very similar energy resolution for both X-ray sources. We also note that the width of the lines is much bigger in both cases as compared to the energy resolution around, for example, the Fe L_3 line (about 1.3 eV at 708 eV). We therefore attribute the extra broadening partly to the lower degree of circular polarization used at BESSY, in combination with the exchange splitting broadening as was observed earlier for different structural phases of Fe (Hunter Dunn *et al.*, 1996). For the source with a degree of circular polarization of 0.5, one expects transitions to both majority and minority final states, particularly in the case of the weakest ferromagnet. The differences observed in Fig. 4 may also be caused in part by the different degree of the spatial coherence between the two sources, as has been discussed in particular for non-dichroic spectra (Hunter Dunn, Arvanitis, Carr & Mårtensson, 2000; Hahlin *et al.*, 2001). Given these systematic differences between spectra at both sources, a straightforward application of the sum rules for the BL 5.2 data would yield moments that are very different from the known ground-state ones, and very different between the two facilities. This is particularly obvious in the case of the orbital moments, especially for Fe, given the data of Fig. 4, where it is obvious even by simple eye inspection.

We have analysed the BL 5.2 data by excluding the spectral region of *s* symmetry between the L_3 and L_2 lines. Under these conditions, the magnetic moment values obtained from the BL 5.2 spectra by applying the MCXD sum rules are found to be higher than the known 'ground state' values of the corresponding bulk phases. This effect had been observed for similar samples characterized at BESSY I (Arvanitis *et al.*, 1996). In the earlier analysis of BESSY data, following the literature, the total dichroic spectral areas were included. The values obtained for the orbital moments, by excluding the *s*-state areas, are 0.2 μ_B per atom for the Ni film and 0.3 μ_B per atom for the Co film. For the spin moments, the values of 0.9 μ_B per atom for the Ni film and 1.5 μ_B per atom for the Co film are obtained. The values obtained at BESSY I, for similar *in situ* grown films, are similar to within the 20% accuracy that is generally attributed to the determination of magnetic moments using the sum rules (Arvanitis *et al.*, 1996). In this previous analysis, the effect of the dipolar term in the sum rules was neglected. For a straightforward comparison with these previous results, we also neglect this term here. Systematic dipolar effects in the sum rules need therefore to be considered separately. The especially strong enhancement of the orbital moment as compared to the ground-state values is attributed to the increased contribution of the surface layers. The spectra are measured in the electron yield channel, with an electron effective escape depth of

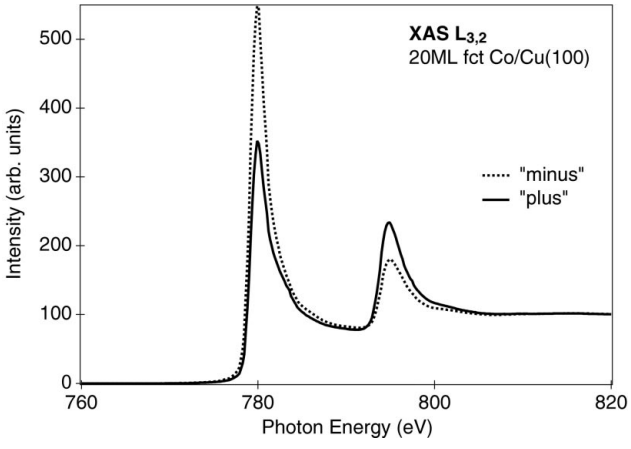

Figure 2
Electron yield spectra of a thick 20 ML Co film at 17° grazing X-ray incidence. The data were collected using BL 5.2 and the EPU (see text). The strong dichroic signal results from the high film quality and the high degree of circular polarization of the EPU, of 0.95 (5). The data were collected at 300 K.

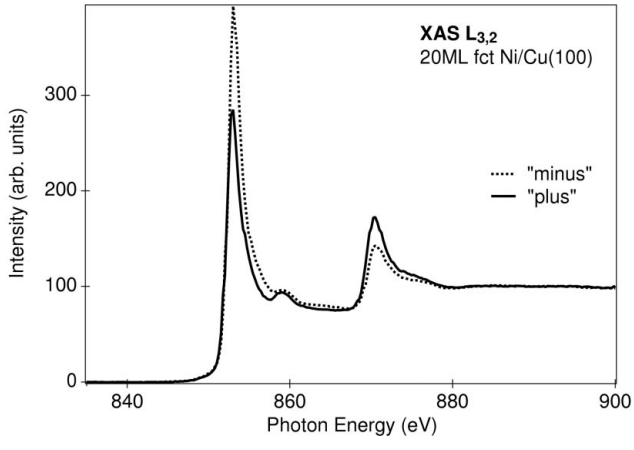

Figure 3
Electron yield spectra of a thick 20 ML Ni film at normal X-ray incidence. The data were collected using BL 5.2 and the EPU (see text). The strong dichroic signal results from the high film quality and the high degree of circular polarization of the EPU, of 0.95 (5). The data were collected at 300 K.

about 17 Å; an enhancement of the orbital moment of up to 100% can be expected for the surface layers (Tischer *et al.*, 1995), leading to the observed increase (Arvanitis *et al.*, 1996).

The previously obtained spin and orbital moments show that within the generally claimed accuracy of the sum rules, of some 20%, transverse coherence effects can be avoided by an appropriate choice of spectral areas in the MCXD difference spectra. This is probably arises from the fact that spectral areas are used only in a relative sense in the sum rules. As they appear in both the nominator and denominator of the corresponding fractions (Carra *et al.*, 1993), the observed intensity enhancements cancel in the first order. However, this situation can only be reached by the exclusion of certain spectral regions. The explicit influence of coherence on spectral intensities indicates that it is not possible to obtain a reliable area transferability of spectral lines measured under different source coherence conditions. Both longitudinal and transverse source coherence are to be considered for an absolute intensity analysis. In particular, the magneto-optic sum rules appear best suited to the case of magnetism applications in a relative sense (Stöhr, 1999), if possible in association with a 'standard'. The present results highlight the importance of performing the measurements of the 'unknown' and the 'standard' compounds under identical spectroscopic conditions. The previous magnetic moment determination shows that the choice of the spectral areas for both the 'unknown' and the 'standard' has to be fixed in a similar way for both compounds. In thin-film research, from the surface-science point of view, a possibility for a convenient determination of the number of holes may be offered by using *in situ* 'standards' of a different electronic nature, such as thin oxide layers (May *et al.*, 1996). However, as no systematic 'coherence' studies on different families of compounds have been reported, it is not clear if spectral line intensities tend always to vary in a similar way, upon increasing source coherence. Previous data comparing data taken at BL 5.2 and SX 700 monochromators for thin, intermediate (a couple of monolayers), and thick (about 20 ML) Fe films indicate that the film thickness is not a sensitive parameter in this context (Hunter Dunn, Arvanitis, Baberschke *et al.*, 2000).

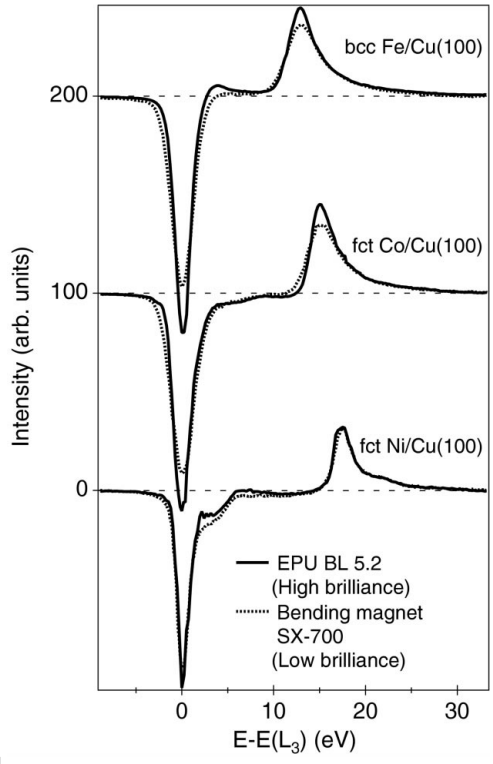

Figure 4
Comparison of data recorded at BL 5.2 and using the SX 700 III beamline at BESSY I for the dichroic parts of the thicker (some 20 ML) Fe, Co and Ni thin films. All spectra are shown with the minimum of dichroic intensity set arbitrarily to an energy of 0 eV on a relative energy scale. An offset of 100 arbitrary units is applied for Co and 200 for Fe, to enable a better comparison to be made. As the EPU delivers light almost fully circularly polarized, scaling factors for the SX 700 data have been used (see text). Clear differences can be observed in the *s*-state spectral region between the two *d*-state white lines. The differences observed in the widths of the white lines are attributed partly to the different degrees of circular polarization of the two sources in combination with the exchange splitting of the final states (see text).

3.2. *Resonant reflectivity*

Figs. 5 and 6 show reflectivity data, taken simultaneously with the electron yield data around the L edges of an ultrathin and a thicker f.c.t. Co film on Cu(100), grown *in situ*. We observe strong dichroic effects, in particular close to the L_3 edge for the 3 and 1.7 ML ultrathin films, and a dramatic change in spectral shape as a function of film thickness. For the 1.7 ML data (Fig. 5), at the L_3 edge, a relative dichroic contrast of 0.8 can be calculated. For electron yield, for 1.7 ML, this value is only about 0.2, indicating the higher absolute sensitivity of resonant reflectivity. Also of relevance is the observation of a reversal of the reflected signal between 0.7 and 1.7 ML. At 0.7 ML, the Co tends to grow in forms of isolated clusters, leading to a film presenting strong roughness. At 1.7 ML, close to the hetero- to homo-epitaxic transition thickness at around 1.8 ML, we are very close to a thickness above which a layer-by-layer growth is observed, and the structural roughness is greatly suppressed (see *e.g.* Tischer *et al.*, 1994). At 3 ML, the Co films can be considered 'flat'. At 0.7 ML, the strong losses in reflected intensity may be attributed to island growth, with non-correlated islands of a characteristic length much smaller than the transverse coherence of X-rays. As the roughness decreases and the sample's structural and magnetic correlation length increases, we find a nonlinear increase of the reflected intensities. We note that interference effects between the various interfaces of thin films and multilayers are reported in the literature. Typically, a Maxwell Fresnel formalism is applied, as in the visible range, to interpret the reflectivity data. Strong intensity variations are

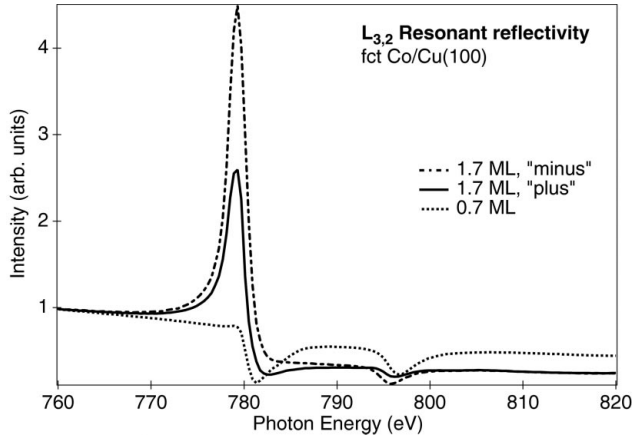

Figure 5
Reflectivity curves recorded at 17° grazing X-ray incidence. The curves are normalized with respect to the signal of the I_0 monitor. They are normalized to unity at the pre-edge region. A nonlinear increase of the reflected signal linked to a change in structure between 0.7 and 1.7 ML is observed. The 1.7 ML data were recollected at a temperature of 96 K. The 0.7 ML showed no dichroism at this temperature.

observed for 3*d*-based thicker films and multilayers, both as a function of the X-ray angle of incidence (see *e.g.* Kao *et al.*, 1994) and thickness (see *e.g.* Rioux *et al.*, 1997). The observation in the present case of a lower reflected intensity above the L_3 edge for the ultrathin films, in contrast to the case of the thicker film, highlights also that interference effects between the reflected beams at the two interfaces are of importance. In this context, we note that it appears natural that the transverse source coherence is of importance for a full description of the reflectivity. Most often, in order to simplify the mathematical formalism, perfect plane waves (infinite transverse coherence) are assumed. In the case of high-quality single-crystalline monodomain samples, such as those investigated here, where the characteristic correlation length describing the crystallographic or magnetic order is of the same order of magnitude or larger than the source coherence volume, such effects should be particularly pronounced. Such a 'scattering' description of the spectroscopic process also offers a natural link to hard X-ray work, where the shorter wavelength allows also for diffraction effects. In this case, the effect of transverse source coherence has been explicitly exploited to obtain holographic information from the diffracted X-ray beams (Robinson *et al.*, 1995). In the hard X-ray region, the link between the absorption and scattering channels has been documented explicitly, for example in the case of diffraction anomalous fine structure oscillations. The present set of data, both in electron yield and reflectivity, indicate that for soft X-rays also, the transverse source coherence needs to be taken explicitly into account for a description of the spectroscopic process.

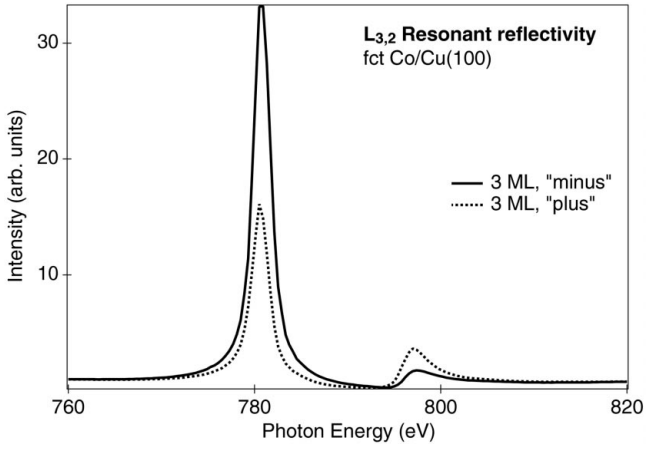

Figure 6
Reflectivity curves recorded at 17° grazing X-ray incidence. The curves are normalized with respect to the signal of the I_0 monitor. They are normalized to unity at the pre-edge region. The data were recorded at 300 K.

The work is supported by the Swedish NFR and TFR Councils and the US DOE.

References

Arvanitis, D., Tischer, M., Hunter Dunn, J., May, F., Mårtensson, N. & Baberschke, K. (1996). In *Spin Orbit Influenced Spectroscopies*, edited by H. Ebert & G. Schütz. Berlin: Springer-Verlag. (See also references therein.)

Carr, R., Kortright, J. B., Rice, M. & Lidia, S. (1995). *Rev. Sci. Instrum.* **66**, 1862–1864.

Carra, P., Thole, B. T., Altarelli, M. & Xindong, W. (1993). *Phys. Rev. Lett.* **70**, 694–697.

Hahlin, A., Karis, O., Brena, B., Hunter Dunn, J. & Arvanitis, D. (2001). *J. Synchrotron Rad.* **8**, 437–439.

Hunter Dunn, J. (1998). *Very Thin magnets: X-rays, Lasers and Spectroscopy*. PhD thesis, Uppsala University.

Hunter Dunn, J., Arvanitis, D., Baberschke, K., Hahlin, A., Karis, O., Carr, R. & Mårtensson, N. (2000). *J. Electron Spectrosc. Relat. Phenom.* **113**, 67–77.

Hunter Dunn, J., Arvanitis, D., Carr, R. & Mårtensson, N. (2000). *Phys. Rev. Lett.* **84**, 1031–1034.

Hunter Dunn, J., Arvanitis, D. & Martensson, N. (1996). *Phys. Rev. B*, **54**, R11157–R11160.

Hunter Dunn, J., Arvanitis, D., Martensson, N., Tischer, M., May, F., Russo, M. & Baberschke, K. (1995). *J. Phys. Conden. Matter*, **7**, 1111–1119.

Kao, C. C., Chen, C. T., Johnson, E. D., Hastings, J. B., Lin, H. J., Ho, G. H., Meigs, G., Brot, J. M., Hulbert, S. L., Idzerda, Y. U. & Vettier, C. (1994). *Phys. Rev. B*, **50**, 9599–9602.

Kortright, J. B., Awschalom, D. D., Stohr, J., Bader, S. D., Idzerda, Y. U., Parkin, S. S. P., Schuller, I. K. & Siegmann, H. C. (1999). *J. Magn. Magn. Mater.* **207**, 1–3.

May, F., Tischer, M., Arvanitis, D., Hunter Dunn, J., Henneken, H., Wende, H., Chauvistre, R. & Baberschke, K. (1997). *J. Phys. IV Fr.* **7**(C2), 389–395.

May, F., Tischer, M., Arvanitis, D., Russo, M., Hunter Dunn, J., Henneken, H., Wende, H., Chauvistrø, R., Märtensson, N. & Baberschke, K. (1996). *Phys. Rev. B*, **53**, 1076–1079.

Rioux, D., Allen, B., Hochst, H., Dai, Z. & Huber, D. L. (1997). *Phys. Rev. B*, **56**, 753–758.

Robinson, I. K., Pindak, R., Fleming, R. M., Dierker, S. B., Ploog, K., Grubel, G., Abernathy, D. L. & Als Nielsen, J. (1995). *Phys. Rev. B*, **52**, 9917–9924.

Stöhr, J. (1999). *J. Magn. Magn. Mater.* **200**, 1–3.

Tischer, M., Arvanitis, D., Aspelmeier, A., Russo, M., Lederer, T. & Baberschke, K. (1994). *J. Magn. Magn. Mater.* **135**, L1–L6.

Tischer, M., Hjortstam, O., Arvanitis, D., Hunter Dunn, J., May, F., Baberschke, K., Trygg, J., Wills, J. M., Johansson, B. & Eriksson, D. (1995). *Phys. Rev. Lett.* **75**, 1602–1605.